

# OSTEOSYNTHESIS PLATE: ANALYTICAL AND FINITE ELEMENT APPROACHES

P. P. Kenedi<sup>\*,\*\*,\*</sup>, L. L. Vignoli<sup>\*\*,\*\*\*</sup>

\* PPEMM- Programa de Pós-Graduação em Engenharia Mecânica e Tecnologia dos Materiais - CEFET/RJ - Av. Maracanã, 229 - Maracanã - RJ - CEP 20271-110 - Brazil

\*\* DEMEC - Departamento de Engenharia Mecânica - CEFET/RJ - Av. Maracanã, 229 - Maracanã - RJ - CEP 20271-110 – Brazil

\*\*\* Mechanical Eng. Dept., Catholic University of Rio de Janeiro, PUC-Rio, R. Marques de São Vicente 225, Gávea, Rio de Janeiro, RJ, Brazil, 22451-900

email: pkenedi@cefet-rj.br

**Abstract:** Osteosynthesis plates have been used to fix broken bones during healing process. The plate is fixed at a long bone, like a human femur by screws, sharing forces and moments with it. In this paper, a plate medial cross section stress distribution was analyzed, through the presentation of an analytical model, mainly based on mechanics of solids. A finite element model was used, as reference, to compare von Mises stress distribution results.

**Keywords:** osteosynthesis plate, stress analysis, analytical model, long bones, finite element model

## Introduction

Osteosynthesis plates (from now on called plates) are used to minimize the recovery period of a patient of fractured long bone, by sharing the bone load, helping the fracture consolidation. Previous works proposes analytical models to estimate load sharing between plate and bone [1]. Mechanics of solids was used to relate external forces, as the joint reaction force and three muscles loads, acting at proximal human femur, with the internal loads acting at a human bone/plate medial cross section. The analytical calculations are presented, in addition to the well-established finite element method, to obtain a better understanding of internal loadings share between bone and plate at a medial cross section.

Figure 1 shows the loading model configuration with four external static forces applied at femur's head, adapted from the Taylor's fourth load case of human left femur's head [2]. The external forces were named: Joint Reaction ( $P_1$ ), Abductors ( $P_2$ ), Iliopsoas ( $P_3$ ) and Ilio-Tibial Tract ( $P_4$ ). See [3] for more complex muscle loading cases description.

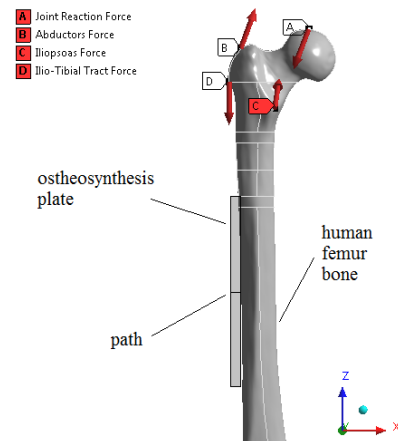


Figure 1: Schematic sketch of a femur loading model. Adapted from [1]

Note this external loading model is a simplification of real human's femur bone external loading.

## Analytical Model

Few hypotheses were used to simplify the mechanical model construction: No bone side ligaments are implemented, the load is shared between plate and bone, the bone and plate cross sections are assumed to be, respectively, hollow circular and rectangular. The screw holes are not modeled. Also the bone tissue is assumed to be cortical and the plate material stainless steel, both supposed as isotropic.

Global and local coordinates systems are considered, as showed at Figure 2. The local axes,  $x$  and  $y$ , follows the cross section centroid of the assembly plate and bone set, and are placed at  $\theta = 180^\circ$ , in counterclockwise direction, relative to the global  $x$  axis ( $x_g$  positive direction is at  $0^\circ$ ).

Figure 2 also shows the bone and plate main cross section dimensions, the reference points at plate cross section area (from 0 to 8) and both coordinate systems.

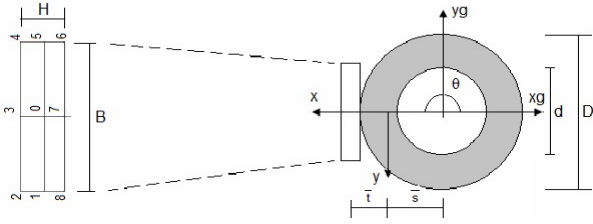


Figure 2: Cross section display for plate at  $\theta = 180^\circ$ .

Expressions 1.a and 1.b shows the distance from bone centroid to bone/plate centroid  $\bar{s}$  and the distance from plate centroid to bone/plate centroid  $\bar{t}$ , according to Figure 2.

$$\bar{s} = \frac{(H+D)}{2 \left(1 + \frac{1}{a^* e^*}\right)} \quad \bar{t} = \frac{(H+D)}{2} - \bar{s} \quad (1)$$

Where  $a^* = A^p/A^b$ ,  $e^* = E^p/E^b$ ,  $b$  and  $p$  superscripts refer, respectively to, bone and plate. Also  $A$  is area;  $E$  is modulus of elasticity.  $B$  and  $H$  are, respectively, the plate width and thickness. The forces and the distances from each force to the cross section centroid can be written in a vector form, using index notation as

$$P_n = P_{n,x_g} \hat{e}_{x_g} + P_{n,y_g} \hat{e}_{y_g} + P_{n,z_g} \hat{e}_{z_g} \quad (2)$$

$$d_n = d_{n,x_g} \hat{e}_{x_g} + d_{n,y_g} \hat{e}_{y_g} + d_{n,z_g} \hat{e}_{z_g} \quad (3)$$

Where,  $g$  subscripts are referenced to global system coordinates.  $\hat{e}_{x_g}$ ,  $\hat{e}_{y_g}$  and  $\hat{e}_{z_g}$  are unit vectors. The index  $n$  ranges from 1 to 4, because of the four external forces. The forces and moments components, written in local coordinates, at centroid cross section are:

$$\begin{pmatrix} V_{n,x} \\ V_{n,y} \\ V_{n,z} \end{pmatrix} = \begin{pmatrix} \cos(\theta) & \sin(\theta) & 0 \\ -\sin(\theta) & \cos(\theta) & 0 \\ 0 & 0 & 1 \end{pmatrix} \begin{pmatrix} P_{n,x_g} \\ P_{n,y_g} \\ P_{n,z_g} \end{pmatrix} \quad (4)$$

$$\begin{pmatrix} M_{n,x_g} \\ M_{n,y_g} \\ M_{n,z_g} \end{pmatrix} = \begin{pmatrix} d_{n,y_g} P_{n,z_g} - d_{n,z_g} P_{n,y_g} \\ d_{n,z_g} P_{n,x_g} - d_{n,x_g} P_{n,z_g} \\ d_{n,x_g} P_{n,y_g} - d_{n,y_g} P_{n,x_g} \end{pmatrix} \quad (5)$$

$$\begin{pmatrix} M_{n,x} \\ M_{n,y} \\ M_{n,z} \end{pmatrix} = \begin{pmatrix} \cos(\theta) & \sin(\theta) & 0 \\ -\sin(\theta) & \cos(\theta) & 0 \\ 0 & 0 & 1 \end{pmatrix} \begin{pmatrix} M_{n,x_g} \\ M_{n,y_g} \\ M_{n,z_g} \end{pmatrix} \quad (6)$$

To get more compact expressions, the stiffnesses are established in Table 1:

Table 1 - Bone and Plate stiffnesses

	Bone	Plate
<b>Axial</b>	$k_a^b = \left( \frac{E^b A^b}{I_c} \right)$	$k_a^p = \left( \frac{E^p A^p}{I_c} \right)$
<b>Bend x axis</b>	$k_{bx}^b = \left( \frac{E^b I_x^b}{I_c} \right)$	$k_{bx}^p = \left( \frac{E^p I_x^p}{I_c} \right)$
<b>Bend y axis</b>	$k_{by}^b = \left( \frac{E^b I_y^b}{I_c} \right)$	$k_{by}^p = \left( \frac{E^p I_y^p}{I_c} \right)$
<b>Torsion</b>	$k_t^b = \left( \frac{4G^b (A^b)^2 t^b}{2\pi R_{med}^b} \right)$	$k_t^p = G^p \left( \frac{1}{3} B H^3 \right)$

Where  $a$ ,  $b$  and  $t$  subscripts refers, respectively to, axial, bend and torsion.  $t^b$  and  $R_{med}^b$  are, respectively, the thickness and the average radius of the bone. For each load, the equivalent stiffness  $k^{eq}$  is compound by bone and plate stiffnesses (springs in parallel arrangement).

The forces and moments are acting at the bone/plate centroid, thus, it is necessary to evaluate load shares. Using geometric compatibility, the displacements and slopes must be the same for plate and bone to ensure the implant stability:

$$N^p = \left( \frac{k_a^p}{k_a^{eq}} \right) \sum_{n=1}^4 V_{n,x} \quad (7)$$

$$V_x^p = \left( \frac{k_{bx}^p}{k_{bx}^{eq}} \right) \sum_{n=1}^4 V_{n,x} \quad (8)$$

$$V_y^p = \left( \frac{k_{by}^p}{k_{by}^{eq}} \right) \sum_{n=1}^4 V_{n,y} \quad (9)$$

$$M_x^p = \left( \frac{k_{bx}^p}{k_{bx}^{eq}} \right) \sum_{n=1}^4 M_{n,x} \quad (10)$$

$$M_y^p = \left( \frac{k_{by}^p}{k_{by}^{eq}} \right) \sum_{n=1}^4 M_{n,y} \quad (11)$$

The torsional stress distribution is modelled through the utilization of a stress function, shown at (16). The stresses are estimated by the following expressions.

The plate axial stress is, [4]:

$$\sigma_{z_{axial}}^p = \frac{N^p}{A^p} \quad (12)$$

The plate bending stresses is, [4]:

$$\sigma_{z_{bend}}^p(x, y) = \frac{M_x^p}{I_x^p} y - \frac{M_y^p}{I_y^p} x \quad (13)$$

The plate transverse shear stresses are, [4]:

$$\tau_{zx_{ts}}^p(x) = \frac{V_x^p Q_y^p(x)}{I_y^p t_y(x)} \quad \tau_{zy_{ts}}^p(y) = \frac{V_y^p Q_x^p(y)}{I_x^p t_x(y)} \quad (14)$$

To model the torsion shear stress, it is used the following stress function [5]:

$$T^p = \sum_{n=1}^4 M_{n,z} \quad \theta_t = \frac{T^p}{k_t^{eq}} \quad (15)$$

$$\phi = \frac{32G^p \theta_t \left(\frac{h}{2}\right)^2}{\pi^3} \sum_{n=1,3,\dots}^{\infty} \left[ \frac{1}{n^3} (-1)^{\frac{n-1}{2}} \left( 1 - \frac{\cosh\left(\frac{n\pi y}{H}\right)}{\cosh\left(\frac{n\pi \frac{b}{2}}{H}\right)} \right) \cos\left(\frac{n\pi x}{H}\right) \right] \quad (16)$$

$$\tau_{zx_t}^p = \frac{\partial \phi}{\partial y} \quad \tau_{zy_t}^p = -\frac{\partial \phi}{\partial x} \quad (17)$$

Also, the stress distributed load along the bone/plate medial contact region is [5]:

$$\sigma_{zcont}^p(x) = -\left( \frac{M_{cont}}{I_y^p} \right) x \quad (18)$$

Where,  $M_{cont} = F_1 l_c / 24$ ,  $F_1$  is the bolt preload,  $I_y^p$  is the moment of inertia relative to the plate centroid and  $l_c$  is the length of the contact between bone and plate. The von Mises criterion was applied to sum the effects of stress distribution caused by each load, [4]:

$$\sigma_z^p(x, y) = \left( \sigma_{z_{axial}}^p + \sigma_{z_{bend}}^p(x, y) + \sigma_{z_{cont}}^p(x) \right) \quad (19)$$

$$\tau_{zx}^p = \tau_{zx_{ts}}^p + \tau_{zx_t}^p \quad \tau_{zy}^p = \tau_{zy_{ts}}^p + \tau_{zy_t}^p \quad (20)$$

$$\sigma_{eq} = \left( \left( \sigma_z^p \right)^2 + 3 \left( \left( \tau_{zx}^p \right)^2 + \left( \tau_{zy}^p \right)^2 \right) \right)^{\frac{1}{2}} \quad (21)$$

See Tab.2, at Appendix, for geometric expressions.

### Numerical Model

The numerical model was built up using the finite element software ANSYS, to simulate the effect of the muscles loads acting on the bone/plate set. The moment and forces resultants were applied at proximal part of tubular structure that represents the bone and the distal part was fixed. The simulations were carried out using the following hypothesis: the bone cross section is hollow circular, the contact between plate and bone is frictionless, the contact between the screw and the bone not allow separation neither slip on their surfaces, screw and plate contact region also is defined as frictionless (the internal surface of the plate hole and the external screw surface are smooth) and the bolt preload is enough to fix the plate [6]. The plate used in this work has  $B = 4.8$  mm,  $H = 16.5$  mm and length  $L = 200$  mm.

The external forces values are (N):  $P_1 = (-1,062; -130; -2,800)$ ,  $P_2 = (430; 0; 1,160)$ ,  $P_3 = (78; 560; 525)$  and  $P_4 = (0; 0; -1,200)$ . The distances between forces point of application and cross section centroid are (mm):  $d_1 = (50.7; -2.7; 218)$ ,  $d_2 = (-13.5; -6.5; 200)$ ,  $d_3 = (18.8; -29.3; 143.7)$  and  $d_4 = (-24.6; -4.2; 168)$ . The cross section bone geometry are  $R_e = 15.5$  mm and  $R_i = 7.65$  mm.

The mesh of the straight plate (0.75 mm) and bone (1.75 mm) are shown at Figure 3. These mesh dimensions was adopted after a convergence study. 1216606 solid elements (SOLID187) and 81854 contact elements (CONTA174 and TARGE170) were used, as well as 1885470 nodes.

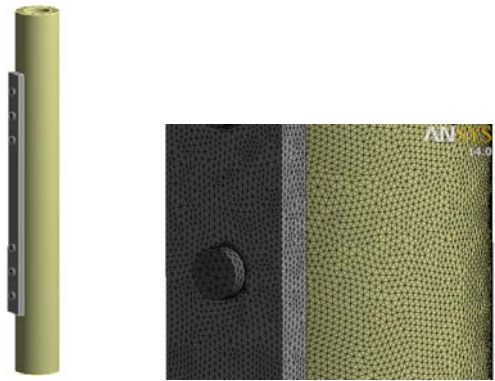


Figure 3: Geometry and mesh of numerical simulation.

The bone was modeled as linear, elastic and isotropic, with  $E^b = 20$  GPa,  $\nu^b = 0.236$ . The plate was modeled with an elastoplastic bilinear behavior with isotropic hardening, with  $E^p = 190$  GPa,  $\nu^p = 0.3$ ,  $S_y^p = 690$  MPa and  $S_{ut}^p = 860$  MPa.

Figure 4 shows plate von Mises stress distribution.

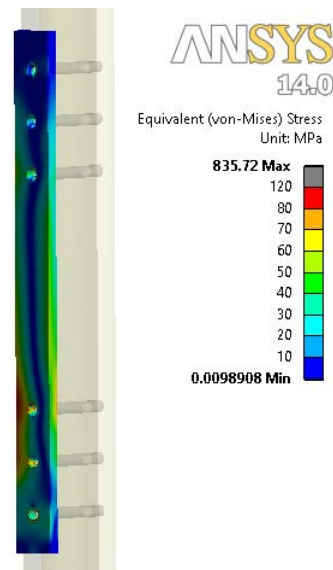


Figure 4: Equivalent von Mises stress of the plate.

**Results**

MathCad software was used to implement the analytical model expressions. As the plate transverse shear stresses were small in comparison to the other stresses, they were not used in analytical model.

To improve the conditions to compare this result with the proposed analytical model, four paths were created at the plate medial cross section edges of Figure 2 and the von Mises stress results were plotted at Figure 5. The path geometry are shown at Figure 2 and are labeled as Path 1, which begin at point 8 and ends at point 2; Path 2, from 6 to 4; Path 3, from 4 to 2 and Path 4, from 6 to 8.

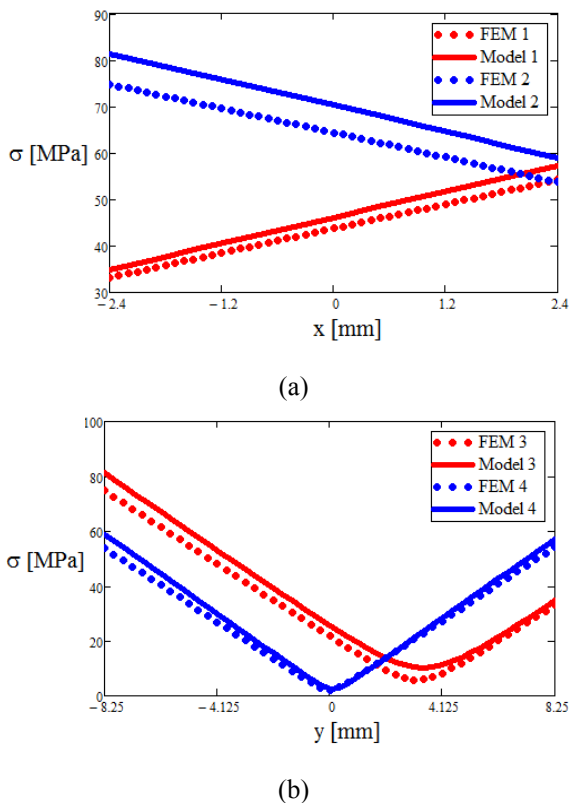


Figure 5: von Mises stress results.

The von Mises results for the four paths plotted, at Figure 5, for analytical and Finite Element models were quite similar, except for path 2. As the stresses were elastic, and the normal stresses were bigger than shear stresses (only torsional stresses are taken into account), the stress distributions were almost entirely linear. Note that path 4 has contact with bone only at  $y = 0$  mm (point 7 of Figure 2). Also note that the slopes change in Figure 5.b is due to Mises stresses components, all squared, so they are always positive. For the adopted loading and distances, at medial cross section, the von Mises stresses varied from 0 to 80 MPa. Points 6 and 4 have the maximum stresses and point 7 has the minimum ones.

**Conclusion**

An analytical model was developed, mainly based on mechanics of solids, to estimate von Mises stress distribution at a plate medial cross section attached to a human femur bone. The explicit relationship between loads and stresses was obtained. The analytical model expressions were implemented on a mathematical software, much cheaper than Finite Element ones, which is an interesting gain. Further developments has to be implement in analytical model, as an upgrade to the plate cross section to better represent a real plate cross section.

**References**

- [1] Kenedi, P.P., Vignoli, L.L., Furtado, L.A., Riagusoff, I.I.T. Osteosynthesis Plate Analytic Model. In Proceedings of the 7th National Congress of Mechanical Engineering – CONEM 2012. Sao Luis, Brazil, 2012.
- [2] Taylor, M.E., Tanner, K.E., Freeman, M.A.R. and Yettran, A.R. Stress and strain distribution within the intact femur: compression or bending? Med. Eng. Phis., Vol.18, nº2, pp. 122-131, 1996.
- [3] Bitsakos, C., Kerner, J., Fisher, I., Amis, A.A. The effect of muscle loading on the simulation of bone remodelling in the proximal femur. J. of Biomechanics, Vol. 38. p. 133-139, 2005.
- [4] Crandall, S.H., Dahl, N.C., Lardner, T.J. An introduction to the Mechanics of Solids. 2nd Edition with SI units, Mc Graw Hill Int. Editions, 1978.
- [5] Timoshenko, S. Strength of Materials. Third Edition, D. Van Nostrand Company. ISSN 2176-54801514, 1955.
- [6] Cordey, J., Borgeaud, M., Perren, S.M. Force transfer between the plate and the bone: relative importance of the bending stiffness of the screws and the friction between plate and bone. Injury, Vol. 31, Suppl. 3, p 21-28, 2000.

**6. APPENDIX**

Table 2 shows geometric expressions used in model.

Table 2: Geometric expressions.

$A^b = \frac{\pi}{4}(D^2 - d^2)$	$A^p = BH$
$I_x^b = \frac{\pi}{64}(D^4 - d^4)$	$I_x^p = \frac{HB^3}{12}$
$I_y^b = \frac{\pi}{64}(D^4 - d^4)$	$I_y^p = \frac{H^3B}{12}$
$I_y^b = I_x^b + A^b \left(\frac{c}{2}\right)^2$	$I_y^p = I_x^p + A^p \left(\frac{t}{2}\right)^2$
$Q_y^b(y) = \frac{H}{2} \left[ \left(\frac{B}{2}\right)^2 - y^2 \right]$	$Q_y^p(x) = \frac{B}{2} \left[ \left(\frac{H}{2} + t\right)^2 - x^2 \right]$
$t_x(y) = H$	$t_y(x) = B$